



OPEN ACCESS

EDITED BY

Ashwini Chauhan,
Tripura University, India

REVIEWED BY

Maged Hassan,
Alexandria University, Egypt
VK Deekshit,
NITTE University Center for Science
Education and Research (NUCSER),
India

*CORRESPONDENCE

Zhaoyan Chen
24707542@qq.com
Ke Wang
keewang@hotmail.com
Jinliang Kong
kj071@163.com

[†]These authors have contributed
equally to this work and share
first authorship

SPECIALTY SECTION

This article was submitted to
Biofilms,
a section of the journal
Frontiers in Cellular and
Infection Microbiology

RECEIVED 10 April 2022

ACCEPTED 22 September 2022

PUBLISHED 12 October 2022

CITATION

Deng W, Lei Y, Tang X, Li D, Liang J,
Luo J, Liu L, Zhang W, Ye L, Kong J,
Wang K and Chen Z (2022) DNase
inhibits early biofilm formation in
Pseudomonas aeruginosa- or
Staphylococcus aureus-induced
empyema models.
Front. Cell. Infect. Microbiol. 12:917038.
doi: 10.3389/fcimb.2022.917038

COPYRIGHT

© 2022 Deng, Lei, Tang, Li, Liang, Luo,
Liu, Zhang, Ye, Kong, Wang and Chen.
This is an open-access article
distributed under the terms of the
[Creative Commons Attribution License
\(CC BY\)](https://creativecommons.org/licenses/by/4.0/). The use, distribution or
reproduction in other forums is
permitted, provided the original
author(s) and the copyright owner(s)
are credited and that the original
publication in this journal is cited, in
accordance with accepted academic
practice. No use, distribution or
reproduction is permitted which does
not comply with these terms.

DNase inhibits early biofilm formation in *Pseudomonas aeruginosa*- or *Staphylococcus aureus*-induced empyema models

Wusheng Deng^{1†}, Yanmei Lei^{1†}, Xiuja Tang^{1†}, Dingbin Li²,
Jinhua Liang¹, Jing Luo¹, Liuyuan Liu¹, Wenshu Zhang¹,
Liumei Ye¹, Jinliang Kong^{1*}, Ke Wang^{1*} and Zhaoyan Chen^{3*}

¹Department of Respiratory and Critical Care Medicine, The First Affiliated Hospital of Guangxi Medical University, Nanning, China, ²Department of Orthopedic Trauma and Hand Surgery, The First Affiliated Hospital of Guangxi Medical University, Nanning, China, ³Intensive Care Unit, The First Affiliated Hospital of Guangxi Medical University, Nanning, China

Anti-infection strategies against pleural empyema include the use of antibiotics and drainage treatments, but bacterial eradication rates remain low. A major challenge is the formation of biofilms in the pleural cavity. DNase has antibiofilm efficacy *in vitro*, and intrapleural therapy with DNase is recommended to treat pleural empyema, but the relevant mechanisms remain limited. Our aim was to investigate whether DNase I inhibit the early biofilm formation in *Pseudomonas aeruginosa*- or *Staphylococcus aureus*-induced empyema models. We used various assays, such as crystal violet staining, confocal laser scanning microscopy (CLSM) analysis, peptide nucleic acid-fluorescence *in situ* hybridization (PNA-FISH), and scanning electron microscopy (SEM) analysis. Our results suggested that DNase I significantly inhibited early biofilm formation in a dose-dependent manner, without affecting the growth of *P. aeruginosa* or *S. aureus in vitro*. CLSM analysis confirmed that DNase I decreased the biomass and thickness of both bacterial biofilms. The PNA-FISH and SEM analyses also revealed that DNase I inhibited early (24h) biofilm formation in two empyema models. Thus, the results indicated that DNase inhibited early (24h) biofilm formation in *P. aeruginosa*- or *S. aureus*-induced rabbit empyema models and showed its therapeutic potential against empyema biofilms.

KEYWORDS

DNase, *Pseudomonas aeruginosa*, *Staphylococcus aureus*, pleural empyema, biofilm

Introduction

Pleural empyema is a serious infectious condition of the pleural cavity associated with high morbidity and mortality (Lehtomaki et al., 2020a; Lehtomaki et al., 2020b). There are approximately 80,000 annual cases of pleural infections in the USA and UK combined (Idell et al., 2017). Despite optimal management, outcomes remain poor with a mortality rate of 20% in adults (Elsayed et al., 2018) and 30% in older people (Bedawi et al., 2021). Approximately 80% of pleural infections can be cured with antibiotics and through chest drainage, and the use of combination therapy with a fibrinolytic agent and DNase reduces the frequency of surgical referrals (Rahman et al., 2011); however, 16–27% of the patients treated in this manner end up requiring surgical treatment (Sundaralingam et al., 2021). Antibiotic resistance and biofilm formation are the main challenges encountered when treating pleural empyema.

Biofilms are sessile communities of microbes surrounded by a self-produced polymer matrix (Rybtke et al., 2015). The extracellular polymeric substances (EPS) that form the matrix comprise polysaccharides, proteins, lipids, and extracellular DNA (eDNA). eDNA contributes to the structural integrity of the biofilm matrix, which is essential for bacterial attachment and aggregation in the early stages of biofilm formation (Davide et al., 2021; Panlilio and Rice, 2021). Approximately 80% of bacterial infections are related to biofilms (KaiLing et al., 2022), which are difficult to remove completely. *P. aeruginosa* and *S. aureus* are the most common pathogens in pleural empyema (Bedawi et al., 2019; Hassan et al., 2019; Chen et al., 2021), and *P. aeruginosa* can form biofilms in pleural empyema (Zhang et al., 2020). Microbial cells within biofilms are 10–1000 times more resistant to antibiotics than planktonic bacteria (Sharma et al., 2019). Biofilm-related infections are recalcitrant to clearance by antimicrobials and host defense molecules (Rather et al., 2021), resulting in antibiotic-resistant and chronic infections. Inhibiting biofilm formation is an effective approach to improve antibacterial efforts and increase the susceptibility of pathogens to antimicrobials.

DNase is an endonuclease that cleaves phosphodiester bonds adjacent to pyrimidines to produce polynucleotides with terminal 5'-phosphates. DNase is used to remove DNA from protein and nucleic acid samples (Karygianni et al., 2020). Moreover, DNase promotes the antibiotic susceptibility of biofilm-associated pathogens in infections (Tetz et al., 2009). DNase degrades eDNA in the matrix, weakening it and facilitating antimicrobial diffusion. Studies have shown that DNase can inhibit or degrade biofilms *in vitro* (Farisa Banu et al., 2017; Ramaraj et al., 2020; Srikanth et al., 2021), and possession of DNase coating increases the antimicrobial activity of *S. aureus* biofilm therapy (Meraj et al., 2020). However, whether DNase inhibits biofilm formation in pleural empyema remains unknown.

Treatment with fibrinolytic agents and DNase is recommended for patients with empyema when intrapleural

therapy is being considered (Chaddha et al., 2021). The Multicenter Intrapleural Sepsis Trials (MIST2) (Rahman et al., 2011) results indicated that intrapleural t-PA/DNase therapy improved fluid drainage and reduced the frequency of surgical referral in patients with pleural infection, but the relevant mechanisms remain unclear. In a consensus statement about DNase and fibrinolytic treatments of pleural empyema, it was hypothesized that the deterioration in patients treated with DNase monotherapy may be due to biofilm disruption mediated by DNase in the pleural cavity (Chaddha et al., 2021). A study showed that the combination with DNase therapy was effective against biofilm-associated wound infections and accelerated wound healing (Kumar et al., 2019). Hence, we speculate that DNase can inhibit biofilm formation in pleural empyema.

In this study, we first demonstrated that DNase I inhibited early biofilm formation in *P. aeruginosa* and *S. aureus in vitro*. Next, we established rabbit empyema models induced by *P. aeruginosa* or *S. aureus*, and investigated the inhibitory effects of DNase I on early biofilm formation.

Materials and methods

Bacterial strains and growth conditions

Both *P. aeruginosa* PAO1 and *S. aureus* (ATCC25913) were stored in Luria–Bertani (LB) broth containing 25% glycerol at –80°C. The *P. aeruginosa* was grown in LB, and *S. aureus* was grown in tryptic soy broth (TSB) supplemented with 0.5% glucose. The bacterial suspensions were standardized to an optical density (OD) of 0.1 at 600 nm (Chen et al., 2016). We prepared dilutions of 2 mL LB or TSB with 10^8 colony-forming units (CFU)/mL bacteria [OD = 0.1], and then serially diluted them to 10^6 CFU/mL for further experiments (Zhang et al., 2020).

In vitro experiments

Growth curve

We used a previously described method (Luo et al., 2016) to compare growth curves. Briefly, we obtained overnight cultures of bacterial solutions (OD₆₀₀ = 0.1), and diluted them with sterile phosphate-buffered saline (PBS) to achieve cell suspensions at OD₆₀₀ = 0.05. The suspensions were supplemented with different concentrations of DNase I (1000 U; Baoriyi Biotechnology, Beijing, China) at 200, 100, 50, 25, 12.5, 6.25, and 0 U/mL. DNase I was derived from a nonanimal host, had an activity of 5 U/μL, and was stored at –20°C. We used a 24-well plate to culture the bacterial solution samples. The OD₆₀₀ measurements were taken every 2 h using a microtiter plate reader.

A microtiter plate biofilm formation assay

We used a partially modified staining method based on those in published studies (Lee et al., 2011; Xu et al., 2015). Briefly, the overnight cultures were grown in different concentrations of DNase I (final concentrations specified above) in flat-bottomed 96-well polystyrene plates for 37°C at 24 h. For biofilm quantifications, we gently rinsed off the unadhered bacteria thrice. After drying, we stained each well with 220 μ L of a 0.1% crystal violet stain for 20 min and gently washed the stain off three times with PBS. After drying, we dissolved the bound stain using 33% acetic acid for 20 min, and measured its absorbance value at OD₅₉₅ using a microtiter plate reader.

Biofilm CFU assay

We used a previously described biofilm CFU assay method (Pezzoni et al., 2020). The overnight cultures were grown in 24-well plates for 24 h at 37°C, and we used the same DNase I concentrations specified above. We discarded the liquid medium with bacteria from the wells, and then washed them gently thrice. Next, we thoroughly scraped the biofilms, and determined the total number of CFUs using the serial dilution method.

Staining of eDNA in biofilms

We followed a published eDNA staining method (Farisa Banu et al., 2017). The overnight cultures were inoculated in the absence or presence of DNase I (final concentration = 66.7 U/L) onto 13 \times 13 mm glass slides in a 24-well titer plate. After 24 h of incubation at 37°C, we gently washed the glass slides and stained them with a 20- μ M propidium iodide solution (10 mL; Shanghai Sigma-Aldrich Trading, Shanghai, China). We visualized and photographed the samples under a fluorescence microscope (Nikon eclipse Ni, Tokyo, Japan).

RNA extraction and RT-qPCR assay

To determine the expression levels of quorum sensing (QS) system-related genes, the bacterial strain samples were grown without or with DNase I (final concentration = 66.7 U/L). The total RNA was extracted using RNAiso Plus (Takara Holdings, Kyoto, Japan). Then, 1 μ g of the total RNA was used for cDNA synthesis using the PrimeScript second strand cDNA synthesis kit (cat. RR047A, Takara). Quantitative real-time polymerase chain reaction (RT-qPCR) was performed using SYBR Green II (cat. RR047A, Takara) on a LightCycler 480 II real-time PCR system (Roche) with the specific primers listed in Table S1. The data were analyzed using the $2^{-\Delta\Delta C_t}$ method as previously described (Pfaffl, 2001).

Confocal laser scanning microscopy analysis

We used a previously described biofilm CLSM method (Yu et al., 2022). Briefly, biofilms were grown on confocal Petri dishes for 24 h in the absence or presence of DNase I (final

concentration, 66.7 U/L). After washing the biofilms with sterile PBS, we used the fluorescent LIVE/DEAD BacLight™ bacterial viability kit L13152 (Molecular Probes, Invitrogen, USA) to detect the live and dead cells according to the manufacturer's instructions. The images were captured and processed using Leica LAS X software, Version core 3.5.7 (Leica, Wetzlar, Germany). Biofilm viability was evaluated using the Fiji macro (ImageJ) method as previously described (Mountcastle et al., 2021). Three points were randomly selected for the examination of every sample, and biomass and average thickness were assessed using COMSTAT2.1 software.

In vivo experiments

Animal studies

The Medical Ethics Committee of the First Affiliated Hospital of Guangxi Medical University approved all the animal experiments (NO.2022-KY-E-(079)). Forty-eight healthy New Zealand rabbits provided by the Experimental Animal Center of Guangxi Medical University, weighing 2.5 ± 0.5 kg, were used in this study.

Pleural empyema induction and DNase I treatment

We randomly assigned 16 rabbits to either a *P. aeruginosa* or an *S. aureus* group; next, we randomly subdivided each group into two groups (medication group and control group). The rabbit models were established as published (Zhang et al., 2020) with some modifications. Briefly, all rabbits were anesthetized with pentobarbital sodium. We placed a drainage tube in the chest cavity using a deep venous catheter package. After ensuring that the pleural cavity did not contain air, we injected 2 mL/kg of LB containing *P. aeruginosa* or TSB containing *S. aureus*. Subsequently, we injected 5 mL of DNase I (200 U) or 5 mL of PBS through the catheter. The catheter was rinsed with 2 mL PBS. After 24 h, we sacrificed the rabbits and performed autopsies. All experiments were repeated three times.

Pleural empyema score

Two researchers who did not participate in the experiments scored the pleural empyema by assessing the amounts of pleural effusion, purulent exudate, and pleural adhesion. We used the pleural empyema score points (0–4) to classify the severities of the pleural empyema based on a published method (Zhu et al., 2006).

Histopathological examination

We fixed the specimens in a 10% formaldehyde solution, embedded them in wax blocks, and cut them into slices; followed by hematoxylin and eosin (H&E) staining. Hematoxylin stains

the cell nuclei blue and eosin stains the cell cytoplasm, muscle tissue, and connective tissue red. For each H&E slide, we randomly selected three visual fields for viewing and photographing under a microscope. After imaging, we measured the thickness of the pleural hyperplasia using the ImageJ software (ImageJ 1.52a, Wayne Rasband National Institutes of Health, Bethesda, USA).

Indwelling catheter analysis

We pulled out the indwelling catheters from the chest cavity, and washed the surfaces with sterile PBS. We cut off 3 cm from the end of each catheter and split it into half. One-half was used for crystal violet staining. The catheter was rinsed three times and a half was sheared. Then, one-half of the catheter was stained with crystal violet as described above. The other half of the catheter was placed in 2 mL of sterile PBS for CFU counts. Each catheter half was vortexed for 10 min and sonicated for 1 min to completely remove the biofilm bacterial colonies from the catheter. The solutions containing colonies from each sample were counted using a 10-times dilution method. The values were recorded as lg (CFU/mL).

Peptide nucleic acid fluorescence *in Situ* hybridization

We performed PNA-FISH according to previously described methods (Sladjana et al., 2009; Wei et al., 2019) using two PNA-FISH kits (AdvanDx, MA, USA), the *P. aeruginosa* kit (cat. QFGNRBC1-25) and the *S. aureus* kit (cat. KT001). Briefly, fibrinous depositions were homogenized and then placed on slides. After drying, we placed a fluorescein-labeled PNA probe in a hybridization solution, and incubated it at 55°C for 60 min. Next, we removed the coverslips and washed them in a preheated (55°C) stringent wash solution for 30 min. After that, we added 4',6-diamidino-2-phenylindole (DAPI) for 15 min. We used a fluorescence microscope to view and

photograph the images. After imaging, we used the ImageJ software to measure the red or yellow fluorescence areas.

Scanning electron microscopy analysis

The right pleurae of the rabbits were fixed with 2.5% glutaraldehyde solution at 4°C for 2 h. We washed the specimens with PBS for 10 min each time. Next, we applied 1% osmium tetroxide for 1 h. Subsequently, we washed the specimens with PBS thrice. The specimens were dehydrated serially using a graded ethanol series (50%, 70%, 95%, and 100%). Finally, we immersed each specimen into 100% hexamethyldisilazane, and vacuum dried it. After drying, the specimens were sprayed with an IB3 (IB5) ion-sputtering instrument and we observed them using SEM.

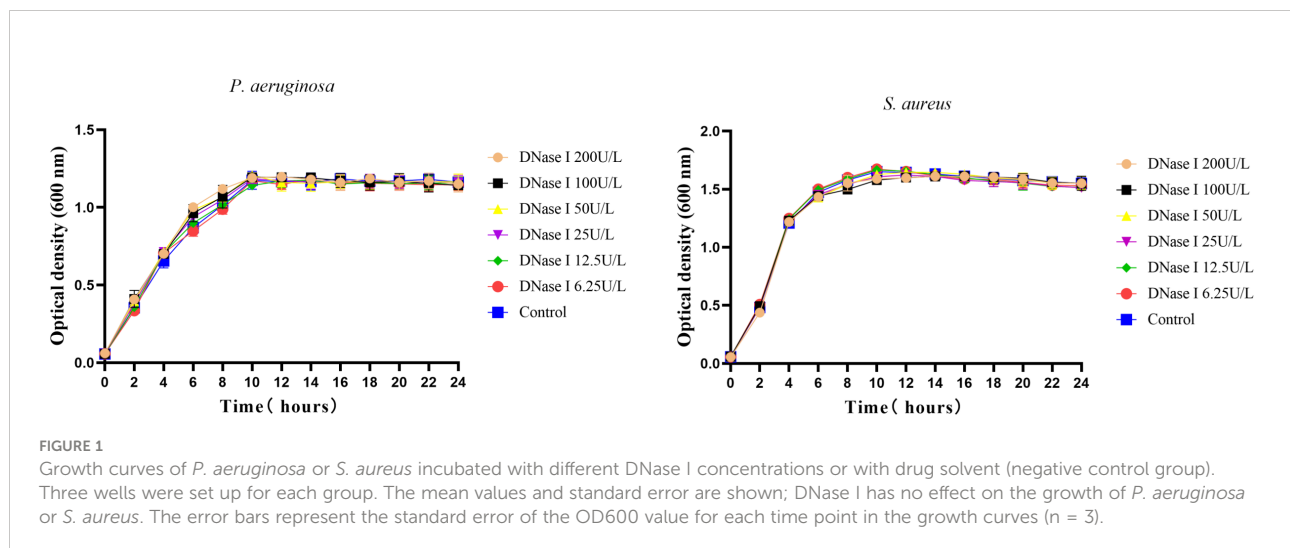
Statistical analysis

We performed all the statistical analyses using the SPSS 22.0 statistical software package (IBM Corp., Armonk, NY, USA). Quantitative variables are expressed as mean \pm standard deviation (SD). Comparisons between multiple groups were conducted using one-way analysis of variance (ANOVA); subsequently, the LSD *t*-test was used for pairwise comparison. Comparisons between two independent groups were performed using the Student's *t*-test. We considered *p*-values < 0.05 as significant.

Results

Growth curves

To assess the effects of DNase I on bacterial growth *in vitro*, *P. aeruginosa* or *S. aureus* were grown in the presence of different dilutions of DNase I. As shown in Figure 1, compared with the control group, different concentrations of



DNase I had no direct bactericidal and bacteriostatic effects on *P. aeruginosa* or *S. aureus* cells.

The biofilm formation assay

To assess the effects of DNase I on biofilm formation *in vitro*, the biofilms were stained with crystal violet, and the ODs were detected. As shown in Figure 2, compared with the control group, different concentrations of DNase I significantly inhibited *P. aeruginosa* or *S. aureus* biofilm formation in a dose-dependent manner ($p < 0.05$).

Biofilm bacterial counts

To assess the effects of DNase I on the growth of biofilm bacteria, we counted the number of biofilm bacteria exposed to different concentrations of DNase I. As shown in Figure 3, compared with the control group, different concentrations of DNase I had no significant effects on the number of *P. aeruginosa* or *S. aureus* in biofilms ($p > 0.05$).

eDNA in the biofilm matrix

To detect the effect of DNase I on the eDNA of biofilm, *P. aeruginosa* or *S. aureus* biofilms were stained with propidium

iodide (which specifically stains eDNA). From the fluorescent micrograph results, it was evident that the control group biofilms had more eDNA accumulation, whereas the DNase I-treated group had less eDNA accumulation (Figure 4).

QS system-related gene expression

The RT-qPCR assay was performed to examine the effect of DNase I on the gene expression of QS systems. As shown in Figure 5, compared with the expression values in the untreated control group, DNase I significantly repressed the transcription level of *lasI* of *P. aeruginosa* ($p < 0.05$); DNase I repressed the transcription levels of *lasR*, *rhlI*, *rhlR*, *pqsA* and *pqsR* of *P. aeruginosa*, but they were not significant ($p > 0.05$). In addition, compared with the expression values in the untreated control group, DNase I significantly repressed the transcription levels of *agrA*, *RNAlII*, and *sarA* of *S. aureus* ($p < 0.05$); DNase I repressed the transcription level of *ica* of *S. aureus*, but it was not significant ($p > 0.05$).

CLSM biofilm image analysis

The antibiofilm activity of DNase I on biofilm formation was also evaluated based on CLSM. As shown in Figure 6, the CLSM images showed a compact biofilm structure in the untreated control group, whereas the DNase I-treated group

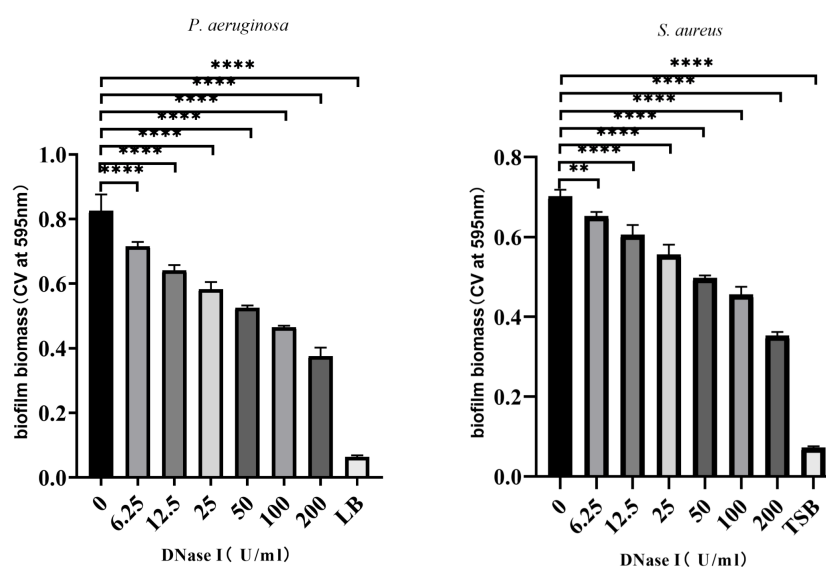


FIGURE 2

DNase I inhibition of biofilm formation by *P. aeruginosa* or *S. aureus* strains. The biofilms were stained with crystal violet and detected by OD₅₉₅ measurements. The results are presented as mean \pm SD. An asterisk indicates a significant difference, ** indicates $p < 0.01$ and **** indicates $p < 0.0001$, compared with the results in the drug-free control group using one-way ANOVA ($n = 3$). ANOVA tests. LB, Luria-Bertani; TSB, tryptic soy broth.

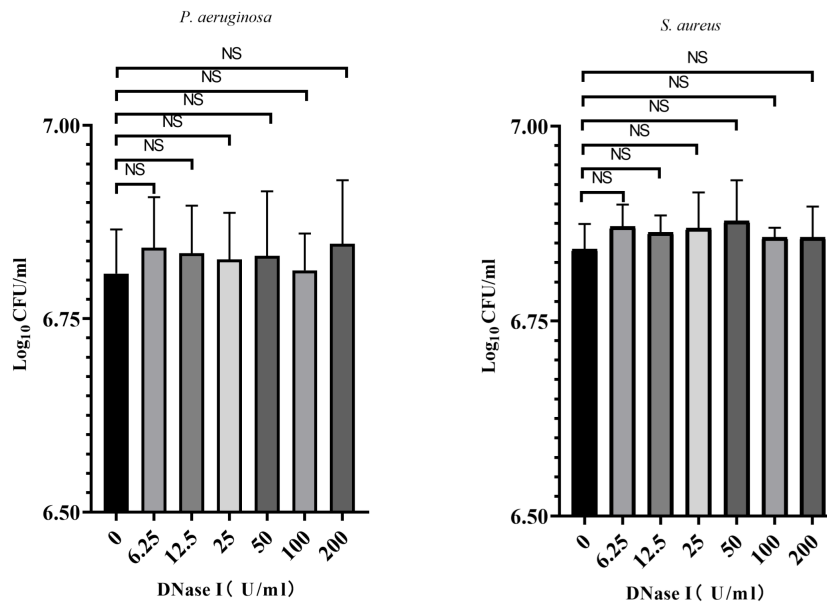


FIGURE 3 Biofilm bacterial counts were obtained after exposure to DNase I for 24 h. The results are presented as mean ± SD. NS indicates *p*-values > 0.05, compared with the results of the drug-free control group using one-way ANOVA (*n* = 3).

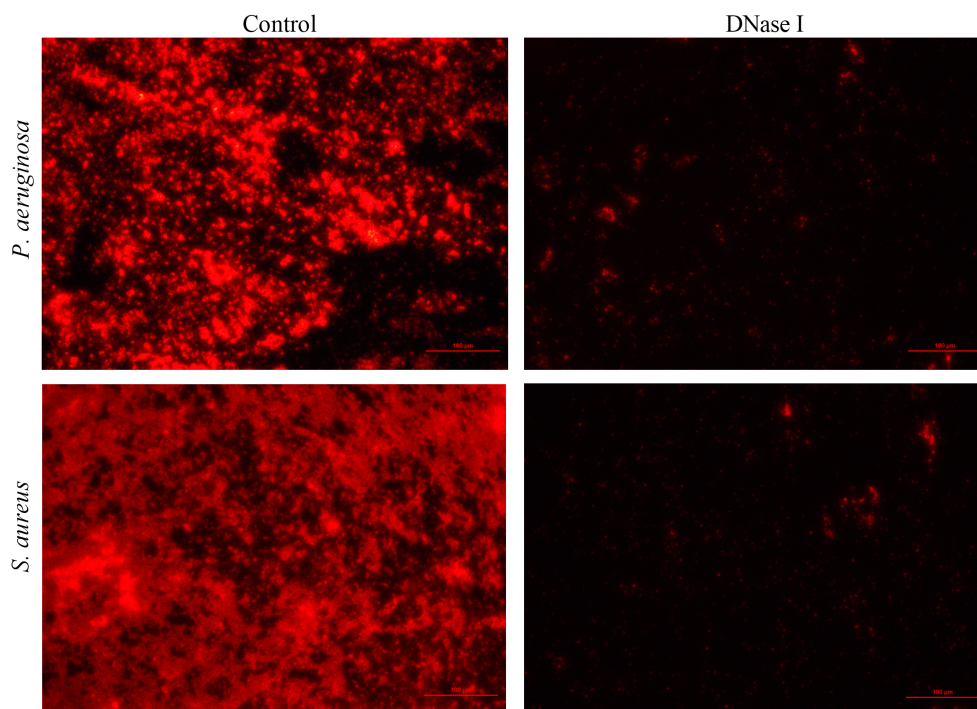


FIGURE 4 Fluorescence microscopy images of *P. aeruginosa* or *S. aureus* eDNA (100×). Propidium iodide (PI)-stained eDNA in red. In the DNase I group, the extent of PI staining decreased compared with the extent in the drug-free control group.

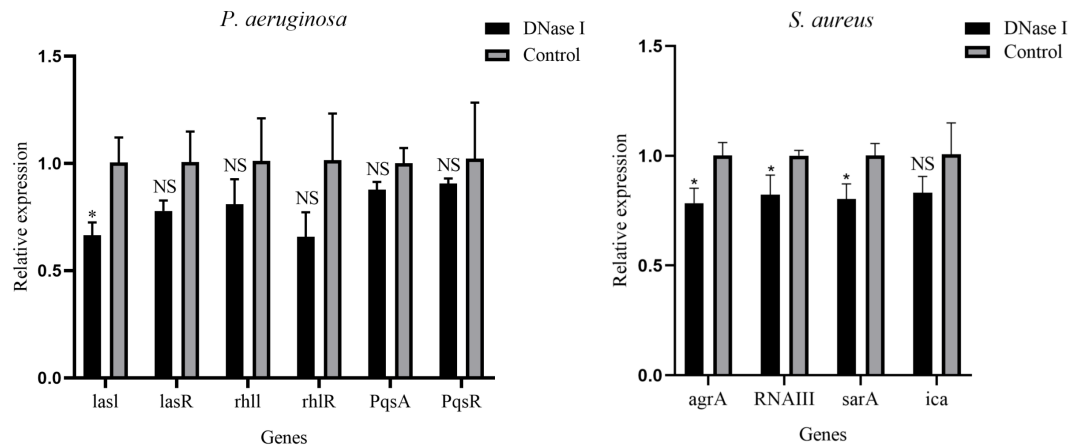


FIGURE 5
Relative expression levels of QS system-related genes of *P. aeruginosa* and *S. aureus* in the presence or absence of DNase I, as determined using real-time polymerase chain reaction. The data are presented as mean \pm SD. An asterisk indicates a significant difference; * indicates $p < 0.05$ and NS indicates p -values > 0.05 , compared with the expression values in the drug-free control group using t -tests ($n = 3$).

was sparse. Compared with the untreated control group, DNase I had no significant effects on the alive cells of *P. aeruginosa* or *S. aureus* in the biofilms ($p > 0.05$). To get more detailed information about the biofilm structure, we analyzed three-dimensional images. DNase I significantly decreased the biofilm biomass as compared with the untreated control group ($p < 0.05$). The mean biofilm thickness of the DNase I-treated group was significantly thinner than those of the untreated control group ($p < 0.05$).

DNase I inhibits biofilm formation in rabbit empyema models

Macroscopic appearance and empyema scores

A total of 48 rabbits were used in our experiments. No animal died in either group. Compared with the DNase I-treated rabbits, the control rabbits showed slightly reduced food and water intakes, normal defecation, lethargy, and reduced activity. On day one after infecting the rabbits with *P. aeruginosa* or *S. aureus*, the control rabbits had more fibrin deposition and more adhesive bands in the pleural cavity than the DNase I-treated rabbits; moreover, the empyema scores of the control rabbits were higher than those of the DNase I-treated rabbits ($p < 0.05$; Figure 7).

Pleural histopathology

To assess the effects of DNase I on the pleural inflammation of empyema, we stained the parietal pleura using H&E staining. We found significant differences in the H&E-stained sections of the rabbit parietal pleura samples between the control and the

DNase I-treated group. In the control rabbits, we observed varying degrees of inflammatory cell infiltrations in the parietal pleura membrane. In the DNase I-treated rabbits, we observed mild inflammatory cell infiltrations. The pleural thicknesses of the DNase I-treated rabbits were significantly thinner than those in the control rabbits ($p < 0.05$; Figure 8).

Biofilm staining on catheter tubes

To assess the effects of DNase I on biofilm formation on catheter surfaces, we stained the biofilms with crystal violet and determined their OD values. As shown in Figure 9, the OD values of the crystal violet staining in the control rabbits were significantly higher than those in the DNase I-treated rabbits ($p < 0.05$).

Catheter bacteriology

To assess the effects of DNase I on catheter colony counts, we diluted the catheter wash solutions and determined the count of viable colonies. Figure 10 shows the colony counts in the control and DNase I-treated rabbits. The catheter colony counts between the control and DNase I-treated rabbits were not significantly different ($p > 0.05$).

Biofilms in the fibrinous deposition of purulent exudate

To investigate the effects of DNase I on biofilms in the fibrinous depositions of purulent exudates, we applied the PNA-FISH method to the samples to detect the ribosomal RNAs of *P. aeruginosa* or *S. aureus* in fibrinous depositions of purulent exudates. In the *P. aeruginosa* control rabbits, the bacteria (red) were surrounded by host cells and the samples showed a bright PNA-FISH signal. In the *S. aureus* control rabbits, the bacteria

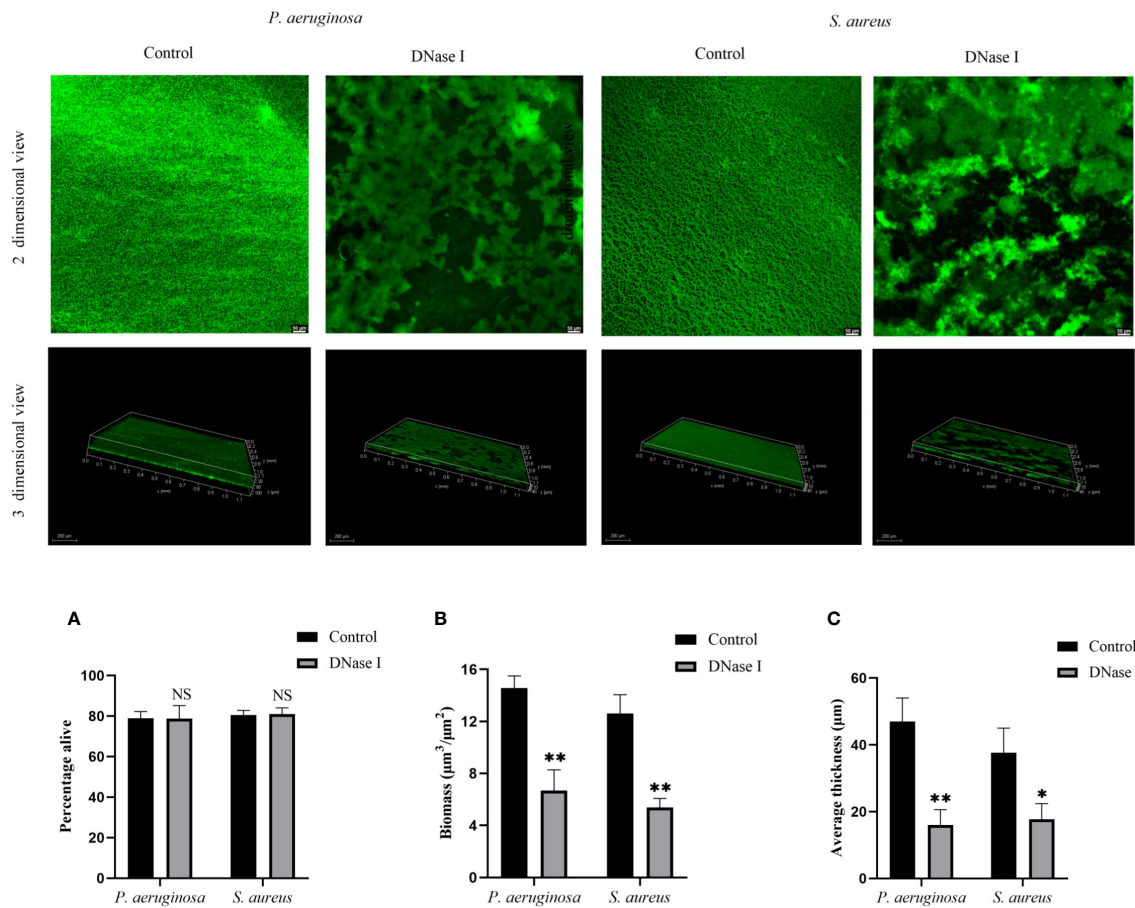


FIGURE 6

Analysis of DNase I effect on the *P. aeruginosa* and *S. aureus* biofilm structures. CLSM analysis of the biofilms formed in the presence or absence of DNase I. The bi-dimensional and three-dimensional biofilm structures were obtained using the LIVE/DEAD[®] Biofilm Viability Kit. Viable bacteria cells with intact membranes are stained fluorescent green. (A) Represents the percentage of live cells. (B) The biofilm biomass of CLSM analysis. (C) Mean thickness of biofilm using CLSM analysis. The data are presented as mean \pm SD. An asterisk indicates a significant difference; * indicates $p < 0.05$, ** indicates $p < 0.01$, and NS indicates p -values > 0.05 , compared with the values in the drug-free control group using t-tests ($n = 3$).

(yellow) were surrounded by host cells and the samples showed a bright PNA-FISH signal. These structures were aggregations. We compared the red or yellow fluorescence areas in each group of rabbits. The areas of the DNase I-treated rabbits were significantly smaller than those of the control rabbits ($p < 0.05$; Figure 11).

SEM evaluation of biofilm formation

To detect the effects of DNase I on biofilm structures in the pleural cavity, we applied the SEM to test samples. We observed biofilm structures on the surface of the pleural membrane formed by microorganisms adhering to the cell surfaces in the control rabbits. The microorganisms were embedded in a self-produced extracellular matrix. Conversely, these structures were absent from the surfaces of the pleural membranes in the DNase I-treated rabbits (Figure 12).

Discussion

Pleural empyema is a life-threatening disease and is associated with the formation of biofilm in the pleural cavity. In a previous study, we were the first to prove that *P. aeruginosa* forms biofilms in a rabbit empyema model (Zhang et al., 2020). In this study, we assessed the effect of DNase I on the inhibition of early biofilm formation *in vitro* and *in vivo*. Our results confirmed that DNase I significantly inhibited the early biofilm formation by *P. aeruginosa* or *S. aureus*. To the best of our knowledge, this is the first study to report DNase inhibits early biofilm formation in pleural empyema.

P. aeruginosa and *S. aureus* cells gradually form an early biofilm from adhesion within 24 h (Tsiry et al., 2015; Jelle et al., 2022). Previous studies have shown that DNase can inhibit or degrade early-stage bacterial biofilm formation *in vitro* (Tetz

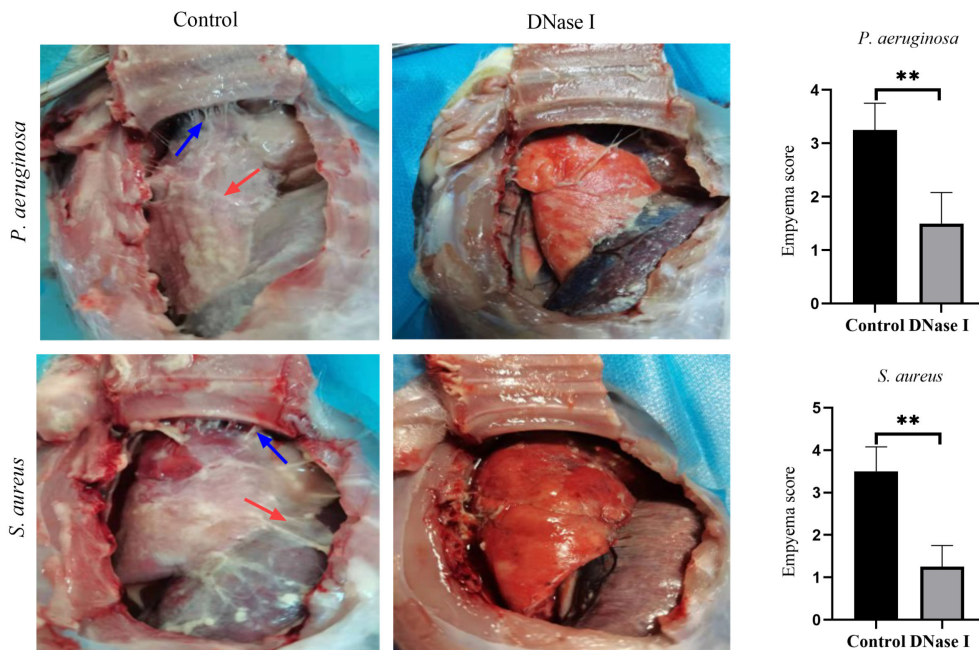


FIGURE 7
Gross pathology specimens of rabbit pleural cavities 24 h after infection and treatment. The control rabbits had more pleural adhesions and fibrin depositions between the visceral and parietal pleura than the DNase I-treated rabbits. The blue arrows indicate adhesion bands and the red arrows indicate fibrin deposition. The empyema scores are presented as mean \pm SD. An asterisk indicates a significant difference; ** indicates $p < 0.01$, compared with the values in the drug-free control group using t -tests ($n = 4$).

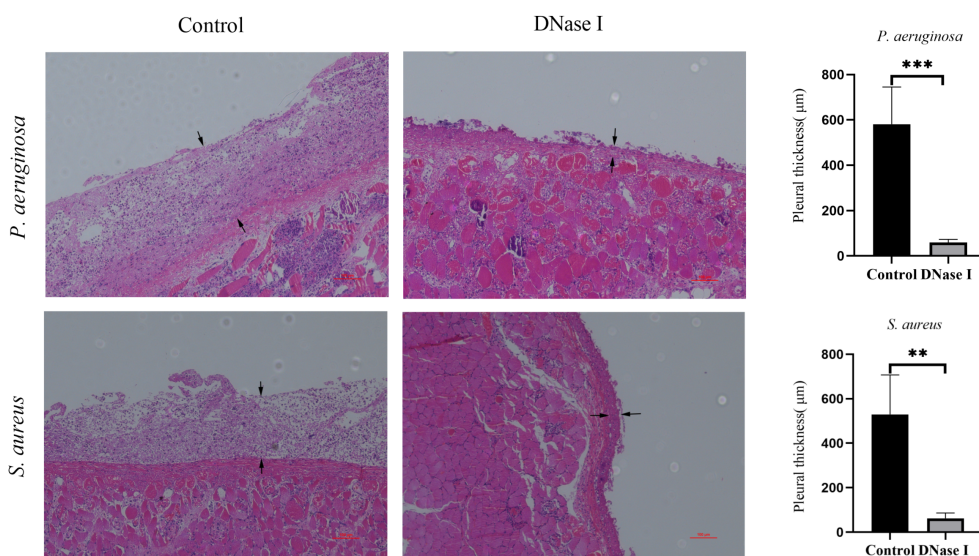


FIGURE 8
Morphological changes of the parietal pleura (H&E staining, 100 \times). The area between the two black arrows is the pleura. In the control rabbits, we observed parietal pleura thickening, accompanied with many inflammatory cell infiltrations. In the DNase-I treated rabbits, the parietal pleura was slightly thickened with only mild inflammation. The pleural thicknesses are presented as mean \pm SD. An asterisk indicates significant difference; ** indicates $p < 0.01$ and *** indicates $p < 0.001$, compared with the values in the drug-free control group using t -tests ($n = 4$).

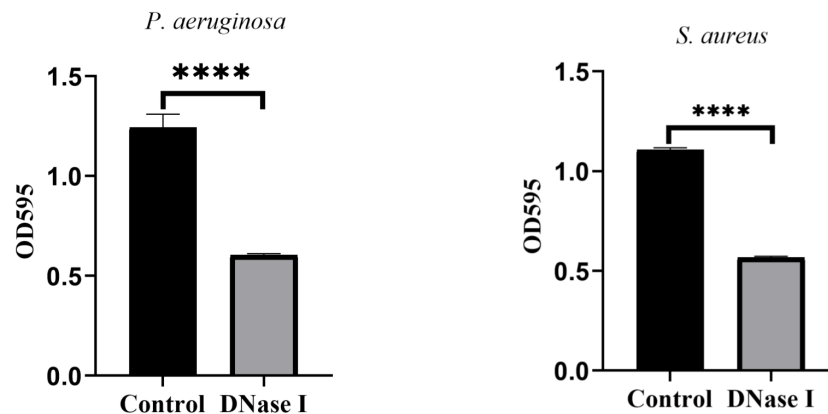


FIGURE 9

Results of the crystal violet staining of the indwelling catheters. OD values of crystal violet staining for indwelling catheters in two rabbit groups. The results are presented as mean \pm SD. An asterisk indicates a significant difference; **** indicate $p < 0.0001$, compared with the values in the drug-free control group using t -tests ($n = 4$).

et al., 2009; Kaplan et al., 2012), and that DNase was an effective treatment strategy against biofilm-associated wound infections (Kumar et al., 2019). In this study, our data reveal that DNase I inhibited early biofilm formation by *P. aeruginosa* or *S. aureus* in rabbit empyema models. The crystal violet staining results suggest that DNase I inhibited early biofilm formation by *P. aeruginosa* or *S. aureus* *in vitro*. More importantly, our PNA-FISH assay and SEM analysis results reveal that DNase I inhibited early biofilm formation in *P. aeruginosa*- or *S. aureus*-induced rabbit empyema models. This finding suggests that the mode of action of intrapleural DNase therapy may be to inhibit early biofilm formation in pleural empyema.

eDNA is known to be important for biofilm stability, and DNase treatment can remove eDNA from biofilms, particularly

during bacterial attachment and the initial stages of biofilm formation (Panlilio and Rice, 2021). Cleavage of eDNA by DNase can promote the penetration of antibiotic molecules and decrease biofilm biomass (Liu et al., 2020). Banu et al. (Banu et al., 2017) found that DNase released eDNA and inhibited *P. aeruginosa* biofilm formation. Our eDNA staining results show that DNase I degraded the eDNA in the biofilm matrix, which was consistent with the results of previous studies (Farisa Banu et al., 2017; Saharut et al., 2020). Thus, these suggest that DNase inhibits early biofilm formation by degrading the eDNA of the extracellular matrix. However, a recent study found that eDNA only localizes outside the matrix rather than inside the biofilm in a murine model infected by *P. aeruginosa* (Alhede et al., 2020). The role of eDNA in pleural

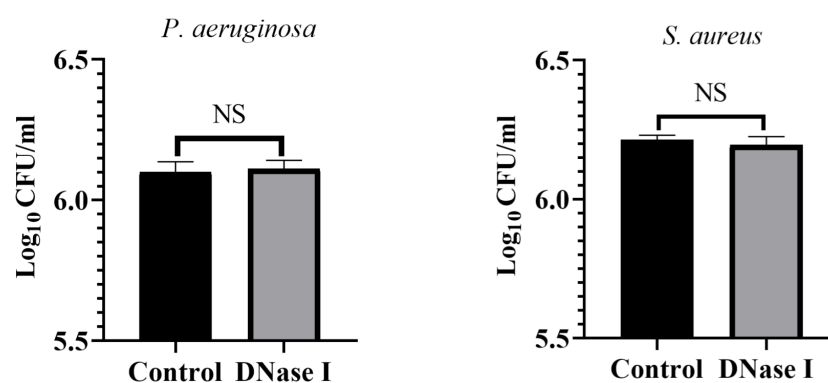


FIGURE 10

Colony counts of the indwelling catheters. Colony counts of *P. aeruginosa* or *S. aureus* on the surface of the indwelling catheters in the two rabbit groups. The results are presented as mean \pm SD. NS indicates a p value > 0.05 , compared with the values in the drug-free control group using t -tests ($n = 4$).

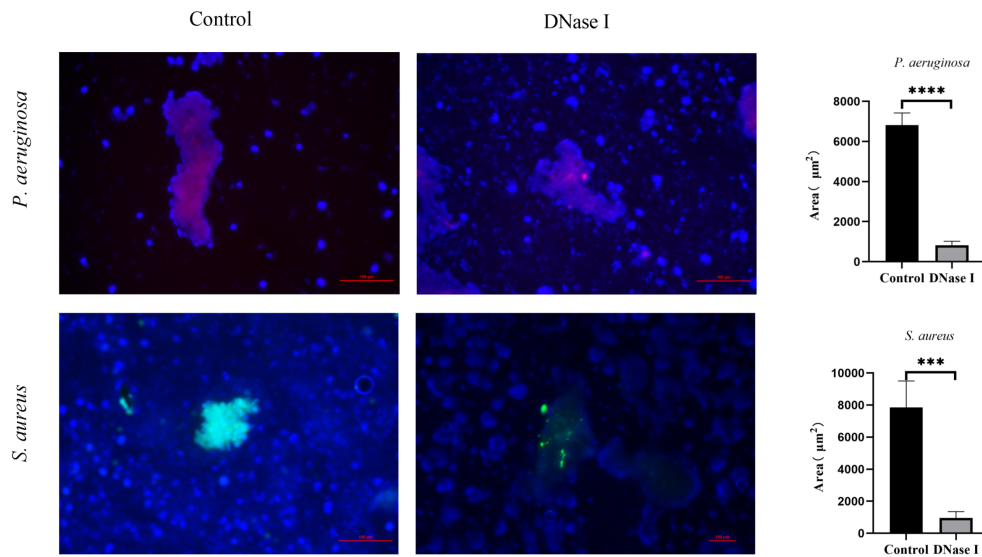


FIGURE 11
 PNA-FISH of fibrinous depositions in purulent exudates (100x). The PNA-FISH kit contained a *P. aeruginosa*-specific probe (red), an *S. aureus*-specific probe (green), and an unspecific nucleic acid stain DAPI (blue) to show the biofilms. The figure shows that the mass bacteria in the control rabbits were surrounded by host cells. The red and yellow portions are the bacterial aggregates surrounded by polymorphonuclear leukocytes. In the DNase I-treated rabbits, few bacteria were surrounded by host cells. We determined the biofilm sizes using PNA-FISH. The results are presented as mean \pm SD. An asterisk indicates a significant difference; *** indicates $p < 0.001$ and **** indicates $p < 0.0001$, compared with the values in the drug-free control group using *t*-tests ($n = 4$).

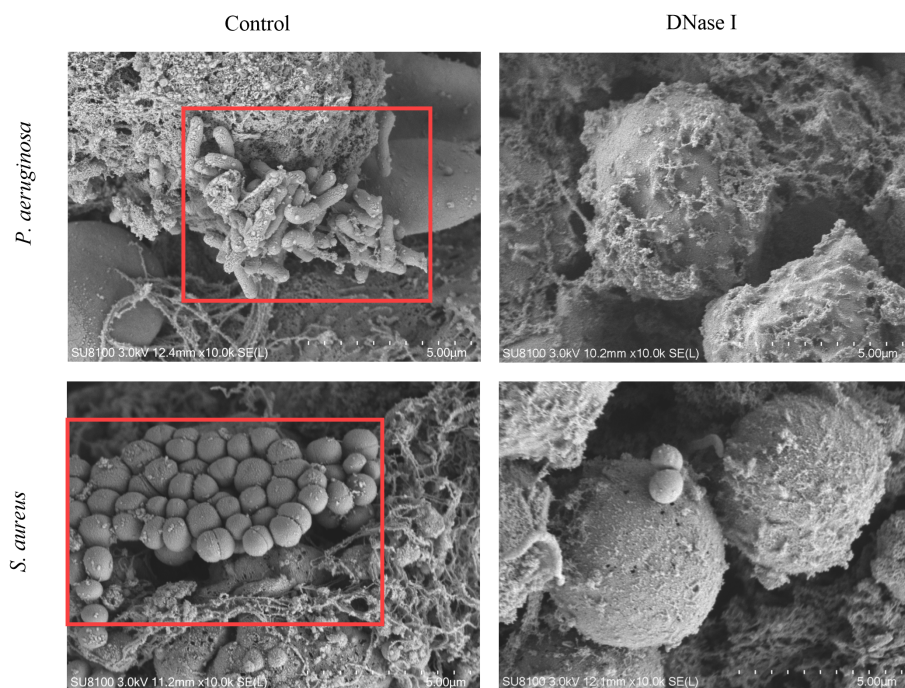


FIGURE 12
 Pleural surface as seen using SEM (10,000x). In the control rabbits, we observed biofilm-like structures on the pleural surface. The *P. aeruginosa* or *S. aureus* strains were embedded in an electron-dense extracellular matrix (red box) in apparent biofilm-like structures. In the DNase-I treated rabbits, we observed only a few bacteria surrounded by a loose matrix.

empyema remains unclear, and we will further investigate this in animal models in the future.

The effect of DNase I on biofilm formation by *P. aeruginosa* or *S. aureus* was further evaluated by observing and analyzing of biofilm using CLSM. The surface morphology and three-dimensional structure of the biofilms could be observed using CLSM (Luo et al., 2018), and CLSM coupled with live/dead fluorescent staining is a powerful tool for the analysis of biofilm structure (Lacotte et al., 2022). The Fiji macro analysis method was used in ImageJ to calculate CLSM bacterial viability, which is an automated image analysis technique that has shown reliable measurements of biomass and cell viability (Mountcastle et al., 2021). Many bespoke software, such as Imaris (Chávez de Paz et al., 2008), COMSTAT (Yin et al., 2022), PHLIP (Lukas et al., 2006), and BiofilmQ (Hartmann et al., 2021), have been used to quantitatively analyze confocal images. Currently, the most widely used biofilm image analysis software in the literature is COMSTAT (Heydorn et al., 2000), which provides the tool to objectively determine the differences in biofilm morphology and parameters for 3D phenotyping. A previous study found out, through CLSM observation and COMSTAT analysis, that DNase reduced the biofilm biomass and average thickness of *P. aeruginosa* biofilm (Farisa Banu et al., 2017), which is consistent with our results. Our COMSTAT analysis results show that DNase I reduced the biomass and average thickness of *P. aeruginosa* or *S. aureus* biofilm. Thus, our CLSM results further confirmed that DNase I inhibited early biofilm formation by *P. aeruginosa* or *S. aureus* *in vitro*.

Our data also show that several QS system-related genes were downregulated upon addition of DNase I to the biofilm formation. Biofilm formation is a complex and unique dynamic process, and the QS system plays an important role in the regulation of genes that control biofilm formation. Chen et al. (Chen et al., 2016) proved that baicalein inhibited *S. aureus* biofilms by downregulating the QS system-associated genes *agrA*, *RNAIII*, *sarA*, and *ica*. Coelho et al. (Coelho et al., 2021) demonstrated that pyranoanthocyanins inhibited biofilm formation and interfered with the expression of the QS system-related genes in *P. aeruginosa* and *S. aureus*. However, there is a lack of research concerning the molecular mechanisms of DNase inhibition in biofilm formation. Our results reveal that the expression levels of several QS system-related genes (*lasR*, *rhlI*, *rhlR*, *pqsA*, *pqsR*, and *ica*) were downregulated after DNase I treatment, but it was not significant. A possible explanation is that biofilm formation is a complex process regulated by multiple pathways, such as the cyclic diguanosine monophosphate, QS system, and *Pseudomonas* quinolone signal. DNase may inhibit biofilm formation through multiple pathways. Our results suggest that one of the mechanisms by which DNase I inhibited biofilm formation by regulating the genes related to the QS-system *P. aeruginosa* and *S. aureus*. The specific mechanisms by which DNase inhibits biofilm formation need to be further studied and discussed.

Biofilms are composed of bacterial communities surrounded by a self-produced polymer matrix that protects them from diverse environmental stresses (Nourbakhsh et al., 2022). eDNA is an important component of the biofilm extracellular matrix (Rajendran et al., 2013), which exists in two forms, namely B-form eDNA (B-DNA) and Z-form eDNA (Z-DNA). B-DNA is found mostly in early biofilms and is sensitive to DNase, but B-DNA turns into Z-DNA in mature biofilms, and this form is resistant to DNase (Buzzo et al., 2021). DNase typically has no apparent effects on mature biofilms (*i.e.*, those growing for > 24 h) (Koo et al., 2017). In addition, studies (Schlafer et al., 2018; Sharma and Pagedar Singh, 2018) have found that DNase is effective against the formation of early biofilms within 24 h, but not after that. Therefore, for this study, we only focused on the early biofilms within 24 h of infection. For mature biofilms (*i.e.*, those growing for 36 h), or earlier biofilms (*i.e.*, those growing for 12 h), we will study the processes of pleural biofilms using multiomics, and to clarify the development of biofilm in different periods in pleural empyema in the future.

Bacterial growth and colony formation are important factors in biofilm formation. Conversely, the biofilms support bacterial growth and protect them from environmental stress. In our study, we found that DNase I had no effect on *P. aeruginosa* or *S. aureus* biofilm bacterial counts *in vitro* and *in vivo*, which is in agreement with results from previous studies (Kaplan et al., 2012; Xu et al., 2015). Karygianni et al. reported that DNase affects the structural integrity and spatial distribution of biofilms, and that it has no effect on the total oral bacteria CFUs (Karygianni et al., 2021). This indicates that DNase acts as an antibiofilm agent, not as an antimicrobial; moreover, clinical experience shows that DNase needs to be combined with antibiotics in the treatment of pleural empyema.

In our study, we found that DNase I decreased the empyema score and it was effective for treating rabbit empyema. Zhu et al. established a rabbit empyema model infected by *Pasteurella multocida* and compared the effect of tPA and rhDNase in the treatment of empyema in rabbits (Zhu et al., 2006). Their study showed that DNase alone was ineffective in decreasing the empyema scores and in treating rabbit empyema. Their results disagree with our experimental results. A possible explanation for this difference is that the antibiofilm effect of DNase decreased with the advancing age of the biofilm; Zhu et al. administered DNase after the diagnosis of empyema, which may be treated because of the mature biofilms; however, DNase I was used for early biofilm in our study. In addition, the complex environment of the chest cavity may also affect the efficacy of DNase. Under the influence of confounding factors, such as pH values and oxygen concentrations in the pleural cavity, the DNase enzymatic activity may vary widely.

For the treatment of pleural empyema, antibiotics and drainage are the first-line therapy (Addala et al., 2021). However, the structure of biofilms better protects bacteria from host defense systems (Krychowiak et al., 2014). In addition, the biofilms seem to

enhance the pathogen's resistance to antibiotics, and unfortunately, the antibiotics we generally use cannot penetrate biofilms to kill bacteria (Hall and Mah, 2017; Wang et al., 2020). Microbial cells within biofilms are more resistant to antibiotics than planktonic cells, which are difficult to remove completely, leading to the emergence of bacterial infections caused by pathogens, such as multidrug-resistant, extensively drug-resistant, and totally drug-resistant bacteria. This is a major cause of persistent inflammation and difficulties in treating chronic infections. Irregular diagnoses and treatments in the clinic may lead to empyema developing into chronic infections. Thus, antibiofilm agents are an option in the management of pleural empyema. Without protection from biofilms, the infecting bacteria may be more exposed to the host immune cells and more easily eliminated (Shang et al., 2022). We found that DNase I inhibited biofilm formation in rabbit empyema models, suggesting that DNase is a potential antibiofilm agent for the treatment of pleural empyema.

Despite continuous progress, understanding of the pathogenesis and management of pleural empyema remains insufficient. In our study, we demonstrated that DNase I inhibited biofilm formation in rabbit empyema models. To some extent, this makes clinical sense. Our PNA-FISH analysis proves that DNase I treatment reduced bacterial aggregation to form biofilms, indicating that DNase may be used for the effective prevention and treatment of chronic empyema infection caused by biofilms. More importantly, DNase inhibits biofilms, which can increase the sensitivity of pathogens to antibiotics, and thus DNase may be used to reduce the use of antibiotics and for the development of resistant bacteria. In addition, intrapleural therapy with DNase does not only reduce the viscosity of the pleural fluid, but also plays the role of an antibiofilm, and thus DNase may be used to improve the removal of bacteria from the pleural cavity. Meanwhile, in a clinical trial, DNase monotherapy was associated with an increase in surgical referrals and provided no fluid-drainage benefit (Rahman et al., 2011); therefore, DNase is recommended with a fibrinolytic agent for adult patients with pleural empyema. However, the optimal dose, duration and timing of DNase treatment for empyema are still not determined, and further studies are needed to elucidate these.

Our study has limitations that should be considered. First, we only observed monotherapy with DNase in the treatment of pleural empyema biofilms. Second, the rabbit sample size of our study was small. Third, although the study provided evidence that DNase was effective to inhibit biofilm formation, we did not investigate DNase therapy on mature biofilms. Finally, empyema is caused by multi-species pathogens, such as *S. aureus*, *P. multocida*, *A. baumannii*, *B. pseudomallei*, and *P. aeruginosa*. Our experiment only focused on a single pathogen in rabbit empyema models, and did not explore mixed pathogen infection. We will investigate mixed pathogen infection of biofilms and mixed pathogen interaction in animal empyema models in the future.

In conclusion, to the best of our knowledge, our study is the first to investigate the inhibition of early biofilm formation in rabbit empyema models by DNase. The results show that DNase significantly inhibited *P. aeruginosa* or *S. aureus* early biofilm formation *in vitro* and *in vivo*. Therefore, DNase inhibits early biofilm formation in *P. aeruginosa*- or *S. aureus*-induced rabbit empyema models and shows its therapeutic potential against empyema biofilm. These results provide a theoretical foundation for the pathogenesis and management of pleural empyema.

Data availability statement

The raw data supporting the conclusions of this article will be made available by the authors, without undue reservation.

Ethics statement

The animal study was reviewed and approved by the Medical Ethics Committee of the First Affiliated Hospital of Guangxi Medical University [NO.2022-KY-E-(079)].

Author contributions

WD, YL and XT conducted the experiments, analyzed the data, and wrote the manuscript. DL and JL participated in the experiments and writing. JL, LL, WZ and LY analyzed the data. KW, JK and ZC designed the study and participated in data analysis and discussion. All authors read and approved the final version of the manuscript for submission.

Funding

This work was supported by the National Natural Science Foundation of China under Grant (No. 82260023, 81760024, 82160783 and 82104499); the Natural Science Foundation of Guangxi Province (No. 2022GXNSFAA035646); the Key Research Program of Guangxi Science and Technology Department (No. AB21196010); the Advanced Innovation Teams and Xinghu Scholars Program of Guangxi Medical University; the Medical Excellence Award Funded by the Creative Research Development Grant from the First Affiliated Hospital of Guangxi Medical University (No. XK2019025); and Partially Supported by Open Funding Project of State Key Laboratory of Microbial Metabolism Of Shanghai Jiao Tong University (No. MMLKF22-06); The Clinical Research Climbing Program Youth Science and Technology Morning Star Program of the First Affiliated Hospital of Guangxi Medical University (No. 201903032 and YYZS2020016).

Conflict of interest

The authors declare that the research was conducted in the absence of any commercial or financial relationships that could be construed as a potential conflict of interest.

Publisher's note

All claims expressed in this article are solely those of the authors and do not necessarily represent those of their affiliated

organizations, or those of the publisher, the editors and the reviewers. Any product that may be evaluated in this article, or claim that may be made by its manufacturer, is not guaranteed or endorsed by the publisher.

Supplementary material

The Supplementary Material for this article can be found online at: <https://www.frontiersin.org/articles/10.3389/fcimb.2022.917038/full#supplementary-material>

References

- Addala, D. N., Bedawi, E. O., and Rahman, N. M. (2021). Parapneumonic effusion and empyema. *Clin. Chest Med.* 42 (4), 637–647. doi: 10.1016/j.ccm.2021.08.001
- Alhede, M., Alhede, M., Qvortrup, K., Kragh, K. N., Jensen, P. O., Stewart, P. S., et al. (2020). The origin of extracellular DNA in bacterial biofilm infections *in vivo*. *Pathog. Dis.* 78 (2). doi: 10.1093/femspd/ftaa018
- Banu, S. F., Rubini, D., Rakshitaa, S., Chandrasekar, K., Murugan, R., Wilson, A., et al. (2017). Antivirulent properties of underexplored cinnamomum tamala essential oil and its synergistic effects with DNase against pseudomonas aeruginosa biofilms – an *In vitro* study. *Front. Microbiol.* 8. doi: 10.3389/fmicb.2017.01144
- Bedawi, E. O., Guinde, J., Rahman, N. M., and Astoul, P. (2021). Advances in pleural infection and malignancy. *Eur. Respir. Rev.* 30 (159). doi: 10.1183/16000617.0002-2020
- Bedawi, E. O., Hassan, M., McCracken, D., and Rahman, N. M. (2019). Pleural infection: a closer look at the etiopathogenesis, microbiology and role of antibiotics. *Expert Rev. Respir. Med.* 13 (4), 337–347. doi: 10.1080/17476348.2019.1578212
- Buzzo, J. R., Devaraj, A., Gloag, E. S., Jurcisek, J. A., Robledo-Avila, F., Kesler, T., et al. (2021). Z-form extracellular DNA is a structural component of the bacterial biofilm matrix. *Cell* 184 (23), 5740–5758.e5717. doi: 10.1016/j.cell.2021.10.010
- Chaddha, U., Agrawal, A., Feller-Kopman, D., Kaul, V., Shojaae, S., Maldonado, F., et al. (2021). Use of fibrinolytics and deoxyribonuclease in adult patients with pleural empyema: a consensus statement. *Lancet Respir. Med.* 9 (9), 1050–1064. doi: 10.1016/S2213-2600(20)30533-6
- Chávez de Paz, L. E., R, H. I., and Gunnel, S. (2008). Oral bacteria in biofilms exhibit slow reactivation from nutrient deprivation. *Microbiol. (Reading England)* 154 (Pt 7):1927–38. doi: 10.1099/mic.0.2008/016576-0
- Chen, Z., Cheng, H., Cai, Z., Wei, Q., Li, J., Liang, J., et al. (2021). Identification of microbiome etiology associated with drug resistance in pleural empyema. *Front. Cell Infect. Microbiol.* 11. doi: 10.3389/fcimb.2021.637018
- Chen, Y., Liu, T., Wang, K., Hou, C., Cai, S., Huang, Y., et al. (2016). Baicalein inhibits staphylococcus aureus biofilm formation and the quorum sensing system *In vitro*. *PLoS One* 11 (4), e0153468. doi: 10.1371/journal.pone.0153468
- Coelho, P., Oliveira, J., Fernandes, I., Araujo, P., Pereira, A. R., Gameiro, P., et al. (2021). Pyranoanthocyanins interfering with the quorum sensing of pseudomonas aeruginosa and staphylococcus aureus. *Int. J. Mol. Sci.* 22 (16):8559. doi: 10.3390/ijms22168559
- Davide, C., Lucio, M., and Renata, A. C. (2021). Extracellular DNA (eDNA): a major ubiquitous element of the bacterial biofilm architecture. *Int. J. Mol. Sci.* 22 (16), 9100. doi: 10.3390/ijms22169100
- Elsayed, H. H., Mostafa, A., Fathy, E., Diab, H. S., Nofal, I. M., AbdelHamid, O. A., et al. (2018). Thoracoscopic management of early stages of empyema: is this the golden standard? *J. Vis. Surg.* 4, 114. doi: 10.21037/jovs.2018.05.18
- Farisa Banu, S., Rubini, D., Rakshitaa, S., Chandrasekar, K., Murugan, R., Wilson, A., et al. (2017). Antivirulent properties of underexplored cinnamomum tamala essential oil and its synergistic effects with DNase against pseudomonas aeruginosa biofilms - an *In vitro* study. *Front. Microbiol.* 8, 1144. doi: 10.3389/fmicb.2017.01144
- Hall, C. W., and Mah, T. F. (2017). Molecular mechanisms of biofilm-based antibiotic resistance and tolerance in pathogenic bacteria. *FEMS Microbiol. Rev.* 41 (3), 276–301. doi: 10.1093/femsre/fux010
- Hartmann, R., Jeckel, H., Jelli, E., Singh, P. K., Vaidya, S., Bayer, M., et al. (2021). Quantitative image analysis of microbial communities with BiofilmQ. *Nat. Microbiol.* 6 (2), 151–156. doi: 10.1038/s41564-020-00817-4
- Hassan, M., Cargill, T., Harriss, E., Asciak, R., Mercer, R. M., Bedawi, E. O., et al. (2019). The microbiology of pleural infection in adults: a systematic review. *Eur. Respir. J.* 54 (3), 1900542. doi: 10.1183/13993003.00542-2019
- Heydorn, A., Nielsen, A. T., Hentzer, M., Sternberg, C., Givskov, M., Ersboll, B. K., et al. (2000). Quantification of biofilm structures by the novel computer program COMSTAT. *Microbiology-Sgm* 146, 2395–2407. doi: 10.1099/00221287-146-10-2395
- Idell, S., Florova, G., Shetty, S., Tucker, T., Idell, R., Koenig, K., et al. (2017). Precision-guided, personalized intrapleural fibrinolytic therapy for empyema and complicated parapneumonic pleural effusions: The case for the fibrinolytic potential. *Clin. Pulm Med.* 24 (4), 163–169. doi: 10.1097/CPM.0000000000000216
- Jelle, V., Qiang, L., Britto, X. B., Sarah, D. B., Matilda, B., Henri, D. G., et al. (2022). The dynamic transcriptome during maturation of biofilms formed by methicillin-resistant staphylococcus aureus&13. *Front. Microbiol.* 13. doi: 10.3389/fmicb.2022.882346
- KaiLing, W., ZhengRong, D., GaoFen, G., HaiFeng, L., Bei, J., and Ying, X. (2022). Anti-larval and anti-algal natural products from marine microorganisms as sources of anti-biofilm agents. *Mar. Drugs* 20 (2), 90. doi: 10.3390/md20020090
- Kaplan, J. B., LoVetri, K., Cardona, S. T., Madhyastha, S., Sadovskaya, I., Jabbouri, S., et al. (2012). Recombinant human DNase I decreases biofilm and increases antimicrobial susceptibility in staphylococci. *J. Antibiotics* 65 (2), 73–77. doi: 10.1038/ja.2011.113
- Karygianni, L., Attin, T., and Thurnheer, T. (2020). Combined DNase and proteinase treatment interferes with composition and structural integrity of multispecies oral biofilms. *J. Clin. Med.* 9 (4), 983. doi: 10.3390/jcm9040983
- Karygianni, L., Paque, P. N., Attin, T., and Thurnheer, T. (2021). Single DNase or proteinase treatment induces change in composition and structural integrity of multispecies oral biofilms. *Antibiotics (Basel)* 10 (4), 400. doi: 10.3390/antibiotics10040400
- Koo, H., Allan, R. N., Howlin, R. P., Stoodley, P., and Hall-Stoodley, L. (2017). Targeting microbial biofilms: current and prospective therapeutic strategies. *Nat. Rev. Microbiol.* 15 (12), 740–755. doi: 10.1038/nrmicro.2017.99
- Krychowiak, M., Grinholc, M., Banasiuk, R., Krauze-Baranowska, M., Glod, D., Kawiak, A., et al. (2014). Combination of silver nanoparticles and drosera binata extract as a possible alternative for antibiotic treatment of burn wound infections caused by resistant staphylococcus aureus. *PLoS One* 9 (12), e115727. doi: 10.1371/journal.pone.0115727
- Kumar, P. K., Bhavya, S. D., Muktanand, T., Meraj, A. M., S. M. M., Ragini, T., et al. (2019). Antibiofilm potential of silver sulfadiazine-loaded nanoparticle formulations: A study on the effect of DNase-I on microbial biofilm and wound healing activity. *Mol. pharmaceutics* 16 (9), 3916–3925. doi: 10.1021/acs.molpharmaceut.9b00527
- Lacotte, P. A., Simons, A., Bouttier, S., Malet-Villemagne, J., Nicolas, V., and Janoir, C. (2022). Inhibition of *In vitro* clostridioides difficile biofilm formation by the probiotic yeast saccharomyces boulardii CNCM I-745 through modification of the extracellular matrix composition. *Microorganisms* 10 (6), 1082. doi: 10.3390/microorganisms10061082
- Lee, J. H., Cho, M. H., and Lee, J. (2011). 3-indolylacetoneitrile decreases escherichia coli O157:H7 biofilm formation and pseudomonas aeruginosa virulence. *Environ. Microbiol.* 13 (1), 62–73. doi: 10.1111/j.1462-2920.2010.02308.x

- Lehtomaki, A. I., Nevalainen, R. M., Toikkanen, V. J., Pohja, E. S., Nieminen, J. J., Laurikka, J. O., et al. (2020b). Pleural infection-an indicator of morbidity and increased burden on health care. *Interact. Cardiovasc. Thorac. Surg.* 31 (4), 513–518. doi: 10.1093/icvts/ivaa147
- Lehtomaki, A., Nevalainen, R., Ukkonen, M., Nieminen, J., Laurikka, J., and Khan, J. (2020a). Trends in the incidence, etiology, treatment, and outcomes of pleural infections in adults over a decade in a Finnish university hospital. *Scand. J. Surg.* 109 (2), 127–132. doi: 10.1177/1457496919832146
- Liu, C., Zhao, Y., Su, W., Chai, J., Xu, L., Cao, J., et al. (2020). Encapsulated DNase improving the killing efficiency of antibiotics in staphylococcal biofilms. *J. Mater. Chem. B* 8 (20), 4395–4401. doi: 10.1039/d0tb00441c
- Lukas, M., Jody, d.B., Jonas, A., Lucas, S., and João, X. (2006). Analysis of a marine phototrophic biofilm by confocal laser scanning microscopy using the new image quantification software PHLIP. *BMC Ecol.* 6 (1). doi: 10.1186/1472-6785-6-1
- Luo, T. L., Eisenberg, M. C., Hayashi, M. A. L., Gonzalez-Cabezas, C., Foxman, B., Marrs, C. F., et al. (2018). A sensitive thresholding method for confocal laser scanning microscope image stacks of microbial biofilms. *Sci. Rep.* 8, 13013. doi: 10.1038/s41598-018-31012-5
- Luo, J., Kong, J. L., Dong, B. Y., Huang, H., Wang, K., Wu, L. H., et al. (2016). Baicalein attenuates the quorum sensing-controlled virulence factors of *Pseudomonas aeruginosa* and relieves the inflammatory response in *P. aeruginosa*-infected macrophages by downregulating the MAPK and NFκappaB signal-transduction pathways. *Drug Des. Devel. Ther.* 10, 183–203. doi: 10.2147/DDDT.S97221
- Meraj, A. M., Kumar, P. K., Deepa, D., Nidhi, P., Ragini, T., Kumar, A. A., et al. (2020). Anacardic acid encapsulated solid lipid nanoparticles for staphylococcus aureus biofilm therapy: chitosan and DNase coating improves antimicrobial activity. *Drug deliv. Trans. Res.* 11 (1), 305–317. doi: 10.1007/s13346-020-00795-4
- Mountcastle, S. E., Vyas, N., Villapun, V. M., Cox, S. C., Jabbari, S., Sammons, R. L., et al. (2021). Biofilm viability checker: An open-source tool for automated biofilm viability analysis from confocal microscopy images. *NPJ Biofilms Microbiomes* 7 (1), 44. doi: 10.1038/s41522-021-00214-7
- Nourbakhsh, F., Nasrollahzadeh, M. S., Tajani, A. S., Soheili, V., and Hadizadeh, F. (2022). Bacterial biofilms and their resistance mechanisms: a brief look at treatment with natural agents. *Folia Microbiol. (Praha)* 67 (4), 535–554. doi: 10.1007/s12223-022-00955-8
- Panlilio, H., and Rice, C. V. (2021). The role of extracellular DNA in the formation, architecture, stability, and treatment of bacterial biofilms. *Biotechnol. Bioeng* 118 (6), 2129–2141. doi: 10.1002/bit.27760
- Pezzoni, M., Pizarro, R. A., and Costa, C. S. (2020). Evaluation of viable cells in *Pseudomonas aeruginosa* biofilms by colony count and Live/Dead staining. *Bio Protoc.* 10 (18), e3762. doi: 10.21769/BioProtoc.3762
- Pfaffl, M. W. (2001). A new mathematical model for relative quantification in real-time RT-PCR. *Nucleic Acids Res.* 29 (9), e45. doi: 10.1093/nar/29.9.e45
- Rahman, N. M., Maskell, N. A., West, A., Teoh, R., Arnold, A., Mackinlay, C., et al. (2011). Intrapleural use of tissue plasminogen activator and DNase in pleural infection. *N Engl. J. Med.* 365 (6), 518–526. doi: 10.1056/NEJMoa1012740
- Rajendran, R., Williams, C., Lappin, D. F., Millington, O., Martins, M., and Ramage, G. (2013). Extracellular DNA release acts as an antifungal resistance mechanism in mature *Aspergillus fumigatus* biofilms. *Eukaryot Cell* 12 (3), 420–429. doi: 10.1128/EC.00287-12
- Ramaraj, S., Kim, M. A., Rosa, V., Neelakantan, P., Shon, W. J., and Min, K. S. (2020). Combined effect of melittin and DNase on enterococcus faecalis biofilms and its susceptibility to sodium hypochlorite. *Materials (Basel)* 13 (17), 3740. doi: 10.3390/ma13173740
- Rather, M. A., Gupta, K., and Mandal, M. (2021). Microbial biofilm: formation, architecture, antibiotic resistance, and control strategies. *Braz. J. Microbiol.* 52 (4), 1701–1718. doi: 10.1007/s42770-021-00624-x
- Rybtko, M., Hultqvist, L. D., Givskov, M., and Tolker-Nielsen, T. (2015). *Pseudomonas aeruginosa* biofilm infections: Community structure, antimicrobial tolerance and immune response. *J. Mol. Biol.* 427 (23), 3628–3645. doi: 10.1016/j.jmb.2015.08.016
- Saharut, W., Sakawrat, K. M., B. J. G., Kamran, N., Suwimol, T., and XXXP., K. B. (2020). DNase-mediated eDNA removal enhances d-LL-31 activity against biofilms of bacteria isolated from chronic rhinosinusitis patients. *Biofouling* 36 (9), 1117–1128. doi: 10.1080/08927014.2020.1857741
- Schlafer, S., Garcia, J., Meyer, R. L., Vaeth, M., and Neuhaus, K. W. (2018). Effect of DNase treatment on adhesion and early biofilm formation of enterococcus faecalis. *Eur. Endod. J.* 3 (2), 82–86. doi: 10.14744/ej.2018.55264
- Shang, Y., Guo, J., Zhao, Y., Chen, J., Meng, Q., Qu, D., et al. (2022). Clemastine inhibits the biofilm and hemolytic of staphylococcus aureus through the GdpP protein. *Microbiol. Spectr.* 10(2), e0054121. doi: 10.1128/spectrum.00541-21
- Sharma, D., Misba, L., and Khan, A. U. (2019). Antibiotics versus biofilm: an emerging battleground in microbial communities. *Antimicrobial Resist Infect Control* 8 (1), 76. doi: 10.1186/s13756-019-0533-3
- Sharma, K., and Pagedar Singh, A. (2018). Antibiofilm effect of DNase against single and mixed species biofilm. *Foods* 7 (3), 42. doi: 10.3390/foods7030042
- Sladjana, M., E, H. K., Anthony, H., L, P. S., W, T. D., and W, W. D. (2009). Detection and identification of specific bacteria in wound biofilms using peptide nucleic acid fluorescence in situ hybridization (PNA FISH). *Microbiol. (Reading England)* 155, 8). doi: 10.1099/mic.0.028712-0
- Srikanth, R., Banu, S. F., Sowndarya, J., Parveen, J. H. S., Rubini, D., Wilson, A., et al. (2021). Biosurfactant synergized with marine bacterial DNase disrupts polymicrobial biofilms. *Folia Microbiol. (Praha)* 66 (5), 831–842. doi: 10.1007/s12223-021-00876-y
- Sundaralingam, A., Banka, R., and Rahman, N. M. (2021). Management of pleural infection. *Pulm Ther.* 7 (1), 59–74. doi: 10.1007/s41030-020-00140-7
- Tetz, G. V., Artemenko, N. K., and Tetz, V. V. (2009). Effect of DNase and antibiotics on biofilm characteristics. *Antimicrob. Agents Chemother.* 53 (3), 1204–1209. doi: 10.1128/AAC.00471-08
- Tsiry, R., Quentin, L., Pierre, D., and Mondher, E. J. (2015). The formation of biofilms by *Pseudomonas aeruginosa*: a review of the natural and synthetic compounds interfering with control mechanisms. *BioMed. Res. Int.* 2015. doi: 10.1155/2015/759348
- Wang, G., Zhao, G., Chao, X., Xie, L., and Wang, H. (2020). The characteristic of virulence, biofilm and antibiotic resistance of *Klebsiella pneumoniae*. *Int. J. Environ. Res. Public Health* 17 (17), 6278. doi: 10.3390/ijerph17176278
- Wei, Q., Zhang, Z., Luo, J., Kong, J., Ding, Y., Chen, Y., et al. (2019). Insulin treatment enhances *Pseudomonas aeruginosa* biofilm formation by increasing intracellular cyclic di-GMP levels, leading to chronic wound infection and delayed wound healing. *Am. J. Transl. Res.* 11 (6), 3261–3279.
- Xu, Q., Sun, F., Feng, W., Liu, X., and Liu, Y. (2015). [Effect of DNase I on biofilm formation of staphylococcus aureus]. *Nan Fang Yi Ke Da Xue Xue Bao* 35 (9), 1356–1359.
- Yin, W. M., Zhang, Z., Shuai, X. X., Zhou, X. D., and Yin, D. R. (2022). Caffeic acid phenethyl ester (CAPE) inhibits cross-kingdom biofilm formation of streptococcus mutans and candida albicans. *Microbiol. Spectrum.* doi: 10.1128/spectrum.01578-22
- Yu, T., Jiang, X., Xu, X., Jiang, C., Kang, R., and Jiang, X. (2022). Andrographolide inhibits biofilm and virulence in *Listeria monocytogenes* as a quorum-sensing inhibitor. *Molecules* 27 (10), 3234. doi: 10.3390/molecules27103234
- Zhang, L., Li, J., Liang, J., Zhang, Z., Wei, Q., and Wang, K. (2020). The effect of cyclic-di-GMP on biofilm formation by *Pseudomonas aeruginosa* in a novel empyema model. *Ann. Transl. Med.* 8 (18), 1146. doi: 10.21037/atm-20-6022
- Zhu, Z., Hawthorne, M. L., Guo, Y., Drake, W., Bilaceroglu, S., Misra, H. L., et al. (2006). Tissue plasminogen activator combined with human recombinant deoxyribonuclease is effective therapy for empyema in a rabbit model. *Chest* 129 (6), 1577–1583. doi: 10.1378/chest.129.6.1577